

Volume 12, issue 3, September 2001 | Articles originaux

A role for interferon-gamma in the hypermetabolic response to murine toxoplasmosis

Abstract

Toxoplasma gondii (Me49 strain) infection into Swiss Webster mice is followed by hypermetabolism and weight loss in the acute phase lasting 14 days. In the subsequent chronic phase of infection, mice showed either a resolution of hypermetabolism and partial weight recovery (Gainers) or persistent hypermetabolism, with stable weight loss (Non-Gainers). The hypermetabolic response was not associated with an augmentation in the thermogenic uncoupling protein 1 (UCP1) mRNA expression in interscapular brown adipose

tissue (BAT), but rather UCP1 expression was reduced. Hypermetabolism is associated with high lipid oxidation as attested by a low respiratory quotient (RQ). Neither BAT nor sympathetic nervous system appear to be involved in the increased lipid utilization, since propranolol did not increase the lower RQ in infected mice. The mitochondrial lipid oxidation blocker mercaptoacetate did not reestablish the respiratory quotient RQ in acute infection (on day 4) and in chronically infected Non-Gainer mice. This suggests an important extra-mitochondrial mechanism of lipid oxidation. Increased lipid peroxidation was detected especially in serum, lung, spleen and liver, which are rich in macrophage-type cells. Following infection peritoneal macrophages exhibited an enhanced capacity to produce reactive oxygen species (ROS). Using IFN-gamma knockout mice we observed that not only the hypermetabolic response was ablated in these mice but there was not a marked increase in ROS production or preferential oxidation/peroxidation of lipids in the acute phase of infection prior to the cachectic phase. The present study described a novel hypermetabolic mechanism involving enhanced lipid peroxidation dependent on IFN-gamma, especially associated with tissues rich in macrophages.

Full text

INTRODUCTION

Infection may result in a wide array of alterations in metabolic activity, which when severe, may lead to a hypermetabolic state eventually leading to the loss of body weight. Peripheral and especially central cytokine expressions are believed to be of importance in infection induced hypermetabolism [1-3]. The effect of central cytokines has been mainly studied in short term protocols using cytokine or bacterial lipopolysaccharide (LPS) injections. Mechanisms by which cytokines induce hypermetabolism depend on individual cytokines. The major pathways of induction of hypermetabolism are believed to be indirect, involving brain receptors, the sympathetic nervous system (SNS) being the main efferent pathway [2] and interscapular brown adipose tissue (BAT) as the major effector in rodents. BAT stimulation leads to the increase in mitochondrial of uncoupling protein 1 (UCP1) expression associated with the liberation of the respiratory chain hence the hypermetabolic response. Interleukins IL-1beta, IL-6 and IL-8 are suggested to act *via* corticotrophin-releasing hormone (CRH). However, not all the cytokines act by this mechanism. Indeed, interferon-gamma (IFN-gamma), tumor necrosis factor alpha (TNF-alpha), IFN-alpha, IL-1alpha do not seem to act

via CRH. Moreover, some studies using infection models suggest that cytokines may also be capable of inducing responses by peripheral mechanisms [4]. It has been shown in sterile turpentine inflammation, in which IL-1beta and IL-6 are mediators, that the hypermetabolic responses are not entirely dependent on the SNS, especially in the later post infection period [5, 6]. Furthermore, in other animal models of infection, not all the hypermetabolisms appear to be associated with increased BAT UCP1 activity [6-8] and SNS activation. Thus the mechanisms underlying infection induced hypermetabolism appears to be complex.

To gain insights into the mechanisms which may underlie cytokine mediated hypermetabolism at "physiological" concentrations, we have conducted a number of metabolic studies using a previously described murine model of toxoplas-mosis [9, 10].

METHODS AND MATERIALS

Mice and diets

Male Swiss Webster (CFW) mice (Charles River, Canada) ~ 2-6 mo of age were used and kept a room temperature (25° C) with a 12:12 hours light/dark cycle. The mice were housed individually in polycarbonate cages and had free access to tap water and standard laboratory chow diet. Knockout male mice and their WT counterparts were 2-6 months of age and were kept as the CFW mice.

T. gondii infection

Mice were injected intraperitoneally with 10 cysts of the Me49 strain of *T. gondii* (obtained from Dr L.L. Johnson,Trudeau Institute, Saranac Lake, NY, USA). During the first week of infection all mice are hypermetabolic compared to controls, but no body weight differences are observed between the two groups [9]. After 7-10 days all mice lost weight and subsequently, the infected mice were classified as G if they showed a partial regain in body weight (about 50% of the infected mice) or NG if they showed no regain after the acute phase of infection [9]. All separate experiments reported here used the design described above. However, since changes in body weight can alter uncoupling protein 1 mRNA expression, metabolic rate and lipid metabolism, we chose therefore to study the interactions of cytokines and *T. gondii* induced hypermetabolism in the first

week of infection where body weight and anorexic effect of infection are not already present.

Cytokine expression in serum, spleen and brain

A previous study showed that TNF-alpha, IL-1beta and IFN-gamma mRNAs were induced rapidly after infection, in association with the hypermetabolic response [9]. These cytokines mRNAs also persisted in chronic phase of infection. Since mRNA levels do not necessarily indicate protein levels, we measured the three cytokines using immunoassays in serum, spleen and brain. Blood was collected retro-orbitally. Tissue cytokine proteins were extracted from the whole organ in 2 ml of 1% 3-((3-cholamidopropyl) dimethylammonio)-1-propanesulfonate in RPMI 1640 medium (Boehringer Mannheim) according to a method described by Nakane [11]. Sera and tissue homogenate supernatants were kept at - 80° C prior to assay. Both tissue and serum cytokines were assayed by immunoassay kits (Quantikine M from R & D) for TNF-alpha, IL-1beta, and IFN-gamma in Swiss Webster mice.

Energy expenditure (EE), respiratory quotient (RQ) and food intake (FI) in wild-type (WT) and knockout mice (KO)

Preliminary assays on serum and tissue cytokines indicated that TNF-alpha and IFN-gamma had a better relationship with hypermetabolic response than IL-1beta. Based on these results we compared the respiratory response to infection in TNF-alpha KO and IFN-gamma KO mice to that of their WT counterparts, to determine the relative importance of these cytokines to infection induced hypermetabolism. UCP1 KO mice were also used to evaluate the role of UCP1 in hypermetabolism following infection. Body weight, FI, EE and RQ were determined for each mouse individually. WT and all KO male mice were obtained from Jackson Laboratory, Maine, USA, whereas male Swiss Webster mice were obtained from Charles River, Canada. KO mice used were IFN-gamma KO - BALB/c-Ifngtm1Ts (12) - mice of Balb/c background, TNF-alpha KO - Tnftm1Gkl [13] - mice with a C57BL6 background, UCP1 KO - Diphtheria toxin A chain FVB/N-TgN(UcpDta) [14] - mice with a FVB/NJ background. Mice were adapted to individual calorimetry cages 3 days before the start of the experiments [15], after this period basal values were obtained as a mean of 3 consecutive days prior to infection or injections. Mice were then injected interperitoneally (ip) with either 10 cysts of *T. gondii*, or vehicle.

Mercaptoacetate, a mitochondrial lipid oxidation inhibitor, was injected ip at 400 micromoles/kg [16]. The percentage of the increase in respiratory rate (VO2) was determined for the 4 hours following the injection and compared to the 2 hours prior to injection. The percentage increase in VO2 over 24 hours was determined by comparing to the average basal VO2 prior to infection. In order to determine the substrate utilisation associated with the hypermetabolic response the respiration quotient (RQ) was calculated.

BAT UCP1 expression

Activation of BAT UCP1 is known to result in hypermetabolism and enhanced lipid oxidation. The expression of UCP1 was followed after infection, to determine if this was the mechanism involved. On days 4, 7, 14 and 28 (G and NG) postinfection *in situ* hybridization histochemistry was performed on BAT to determine the levels of UCP1 in the tissue using a rat UCP-1 probe [17]. *In situ* hybridization histochemistry was performed as previously described [18]. Mice were anesthetized with 0.3 ml of a mixture containing 40 mg/ml of ketamine and 2 mg/ml xylazine. Without any delay mice were perfused intracardially with 20 ml of ice cold isotonic saline followed by 100 ml of a paraformaldehyde (4%) solution. At the end of the perfusion, BAT was removed and kept in 4% paraformaldehyde for an additional 3 to 4 days. Twelve hours BAT were transferred to a solution containing paraformaldehyde and sucrose (10%) for twelve hours and then cut with a sliding microtome (Histoslide 2000, Reichert-Jung). 25 mum thick sections of BAT embedded in paraffin were collected and mounted onto slides. The sections were then successively fixed for 20 min in paraformaldehyde (4%), digested for 30 min at 37° C with proteinase K (10 mug/ml in 100 mM Tris-HCl containing 50 mM EDTA, pH 8), acetylated with acetic anhydride (0.25% in 0.1 M trietholamine, pH 8) and dehydrated through graded concentrations (50, 70, 95 and 100%) of alcohol. After vacuum drying for at least 2 hours, 90 mul of the hybridization mixture, which contained an antisense 35S labeled cRNA probe (10 million cpm/ml), were spotted on each slide. The slides were sealed under a coverslip and incubated overnight at 60° C in a slide warmer. The next day, the cover slips were removed and the slides rinsed four times with 4X SSC (0.6 M NaCl, 60 mM sodium citrate buffer, pH 7), digested for 30 min at 37° C with RNAase-A (20 mug/ml in 10 mM Tris-500 mM NaCl containing 1 mM EDTA, washed in descending concentrations of SSC (2X, 10 min: 1X, 5 min: 0.5X, 5 min: 0.1X, 30 min at 60° C), and dehydrated through graded concentrations of alcohol. After a 2 hour period of vacuum drying, the slides

were exposed on a X-ray film (Eastman Kodak, Rochester, NY) for 24 hours. Once removed from the autoradiography cassettes, the slides were defatted in xylene and dipped in NTB2 nuclear emulsion (Eastman Kodak). The slides were exposed for 7 days before being developed in D19 developer (Eastman Kodak) for 3.5 minutes at 14-15° C and fixed in rapid fixer (Eastman Kodak) for 5 min. Finally tissues were rinsed in running distilled water for 1 to 2 hours, counterstained with thionin (0.25%), dehydrated through graded concentrations of alcohol, cleared in xylene and coverslipped with DPX. The specificity of the antisense riboprobe was strongly suggested by the absence of a positive signal in sections hybridized with the sense probe.

Northern blots for UCP1 were performed as previously described [19] and coloration of membrane showed equal loading. Weight matched mice are non infected mice which are underfed to have the same body weight as infected G or NG, were used to dissociate possible hypophagia effects on UCP1 mRNA expression.

Peritoneal macrophage ROS production

Hypermetabolism and increased lipid oxidation did not appear to be associated with enhanced UCP1 expression following infection. Further studies involving the beta-blocker propranolol (data not shown) had no significant effect, nor did the mitochondrial beta-oxidation inhibitor mercaptoacetate. Oxidation of lipids therefore arose from non-mitochondrial sources. Reactive oxygen species are capable of oxidizing lipids, therefore we followed the capacity of peritoneal macrophages to produce ROS following infection. Briefly, peritoneal macrophages were isolated by injecting sterile pyrogen free phosphate buffer saline - PBS (ICN, Canada). Cells were resuspended in PBS and 10^5 were aliquoted to each well in a 96 well tray and left to adhere for 1 hour. After this time period cells were gently washed with 100 mul of PBS 2X. After the final wash, 100 mul of nitro blue tetrazolium (NBT) in PBS - 5% glucose was added and cells were incubated for 3 hours. Following this incubation at 36° C, the supernatant was removed and cells gently washed with PBS. Cells were then fixed with 70% methanol and left to dry. The insoluble reduced NBT was solubilized by adding 100 mul of 2M KOH and 100 mul DMSO. The OD was then measured at 630 nm within 30 min [20].

Lipid peroxidation in sera and tissue

To measure lipid peroxidation in sera and tissues, the Biotech LPO-586 colorimetric assay kit and its protocol (Oxis, Portland, USA) was used. Briefly, animals were perfused with saline for 3 min at 4° C. Tissues were homogenized to give a 30% solution (*i.e.* 3 g of tissue in 10 ml of buffer) in 20 mM Tris buffer pH 7.4 containing 5 mM butylated hydroxytoluene. Homogenate was then centrifuged at 4° C to remove cellular debris. Aliquots were then taken for determination of malondialdehyde (MDA) using the methanesulfonic acid solvent procedure. Absorbance was measured at 586 nm and corrections were made for sample and reagent blanks. Concentrations were then determined using a standard curve.

Data analyses

All data are presented as mean ± SD. Statistical analyses were performed using Kruskal-Wallis one way nonparametrical AOV. P value less than 0.05 was considered significant.

RESULTS

Body weight following infection

In the acute phase following infection all mice were hypermetabolic, this was followed by weight loss and then by a stabilisation of body weight. We have shown in a previous study [9] that in the chronic phase, only those mice that showed no regain in body weight (NG) remained hypermetabolic compared to their weight-matched non infected controls. Infection with *T. gondii* can result in small variations in survival. However the ratio of mice that show a partial body weight regain (Gainers) compared to those that do not (non Gainers) appears to be relatively constant (50%) in different experiments.

In this particular experiment with 10 mice were infected with 10 cysts, 4 mice became Gainers and 6 became Non Gainers (Figure 1).

Role of UCP1 in BAT following infection

UCP1 mRNA expression was found to be down regulated following infection as quantified by northern blots (Figure 2). These results also show that body weight loss due to anorexia independent of infection (*i.e.* in weight matched -

WM - controls) can lead to decreases in UCP1 mRNA expression. We have therefore foccused our studies, in particular on day 4 after infection where hypermetabolism is already maximal but no body weight loss occurs. Using day 4 after infection we eliminate factors that may influence metabolic rate and substrate utilisation due to loss of body weight and reduced food intake. *In situ* hybridisation also confirmed down-regulation of BAT UCP1 expression (Figure 3) following infection compared to control BAT. Although infection results in the infiltration of immune cells into BAT, the reduction of UCP1 mRNA did not appear to be in the specific vicinity of the immune cells. UCP1 therefore did not appear to mediate the hypermetabolic response to *T. gondii.* This conclusion is further substantiated by the findings that the hypermetabolic response to *T. gondii* still occurred in UCP1 KO mice as did the increased lipid oxidation response (Table 1).

Cytokine production in serum, spleen and brain

IL-1beta: during the first week, IL-1beta was not detected in the serum and brain (Figure 4 top panel).

TNF-alpha: TNF-alpha was detected at the onset of infection and hence was associated with the onset of the hypermetabolic response (Figure 4 middle panel). From day 1 post infection, there was a significant increase in TNF-alpha in the spleen from 1,129 ± 140 pg/ml in control animals vs 2,495 ± 166 pg/ml in infected animals, p 0.03), TNF then remained elevated in all subsequent phases in infected animals. No significant difference was seen between the spleen of G and NG (2,113 ± 312 pg/ml and 2,273 ± 358 pg/ml respectively).

TNF was not detected in the brains of control mice. No significant difference was observed in the chronic phase in the brain 787 ± 106 pg/ml and 855 ± 109 pg/ml in G and NG respectively.

IFN-gamma: IFN-gamma was not detected in any tissues of control mice. As seen in Figure 4 bottom panel, serum IFN-gamma was found to be increased at the onset of infection (60 pg/ml) and further elevated on day 7 and 14 (165 ± 10 pg/ml and 212 ± 10 pg/ml respectively). In the brain, there were increases in IFN-gamma on day 7 and 14 (33 ± 6 pg/ml and 18 ± 2 pg/ml respectively). In the chronic phase of the infection, the serum cytokine level was reduced in the G (below detection level) but remained markedly elevated in the NG (67 ± 10 pg/ml) subgroup. Furthermore in the chronic phase, there was a drastic 10-fold

increase in brain IFN-gamma in the NG (224 ± 8 pg/ml) compared to the low levels observed in the G subgroup (20 ± 2 pg/ml). In the spleen NG had a 2 fold increase compared to G (134 ± 11 and 69 ± 5 respectively). IFN-gamma therefore has a better relationship with the hypermetabolic and cachexic state than the other cytokines measured.

Infection-induced hypermetabolism in WT, TNF-KO, IFN-KO and UCP1 KO mice

WT, TNF-alpha, IL-6 KO (data not shown) and UCP1 KO mice all demonstrated a hypermetabolic response to *T. gondii* compared to their wild-type counterparts during the first week of infection (Figure 5). In contrast IFN-gamma KO mice showed no increase in VO2 in response to *T. gondii* infection where as their WT counterparts did (Figure 5). The hypermetabolic response (increase in VO2) does not appear to vary largely with the different genetic background of the mice. In these studies with WT counterparts of the KO which showed hypermetabolic responses in the acute 7 day phase of *T. gondii* infection but no weight loss occured. It should be noted that after this phase some

of the infected WT showed weight loss where as others did not, this was associated with strain resistance differences.

Respiratory Quotients (RQ)

Examination of the respiratory quotients (RQ) data revealed that this variable was decreased in mice that showed a hypermetabolic response to *T. gondii* in the acute phase (day 4, 7, 14) and in NG (day 28). IFN-gamma KO mice showed no change either in VO2 or in RQ (Table 1) on day 4 post-infection. IFN-gamma was associated not only with the hypermetabolic response to *T. gondii* but also with selective fuel oxidation. Note that neither propranolol (data not shown) or mercaptoacetate increased the RQ of infected mice (see below) this is consistent with our findings that UCP1 is not implicated in the hypermetabolic effect.

Lipid peroxidation by non-mitochondrial mechanisms

In order to gain insights into the mechanisms underlying the enhanced lipid oxidation (decreased RQ), the *T. gondii* infected mice were treated with an

inhibitor of mitochondrial beta-oxidation (mercaptoacetate), on day 4 post infection, as well as in the NG. As expected, the RQ increased in the control (indicating a decrease in lipid oxidation), but no increase in RQ was seen in the infected mice. On day 4 infected mice had a RQ of 0.83 ± 0.02 compared to 0.81 ± 0.02 of mercaptoacetate treated infected mice; this difference is not significant. In the chronic phase of infection NG had a RQ of 0.77 ± 0.02, mercaptoacetate treated NG had a RQ of 0.74 ± 0.02. Consequently, the decrease in RQ during cachexia both in the acute and chronic phases could not be due solely to mitochondrial beta-oxidation, but to some other processes. Reactive oxygen species (ROS) are capable of oxidising lipids, therefore we followed the capacity of peritoneal macrophages to produce ROS.

As shown in Figure 6, ROS production was increased markedly (about 5-fold) during the acute phase (day 1, 4, 7, 14), but during the chronic phase it was reduced compared to control levels in the NG, and even below control levels in the G (however compensations in lipid peroxidation occurs in other tissues - Figuure 7). IFN-gamma was required to activate macrophages to produce ROS (Figure 6), and infection may therefore increase lipid peroxidation by ROS dependence on IFN-gamma. Changes in lipid peroxidation in various tissues and ROS production in macrophage in this model of *T. gondii* infection were investigated.

The data on indices of lipid peroxidation are presented in Figure 7 and indicate that these were increased during both the acute and chronic phases. Parallel changes were observed in the sera, lung and spleen, and to a lesser extent in the liver, but evidently not to the same degree in the brain. It should be noted that the importance of the sites of lipid peroxidation are dependent on the time after infection, as is observed in the differences between the acute and the chronic phase.The levels of lipid peroxidation - malondialdehyde (MDA) in IFN-gammaKO mice remained comparable to the non infected control but was always significantly reduced compared to infected mice on the same day ($p < 0.01$) in various tissues (Figure 7).

Taken together, these results indicate the importance of altered macrophage ROS production during the acute phase and that of changes in lipid peroxidation in the lung and spleen in both acute and chronic phases.

The possible importance of IFN-gamma in these elevations in ROS and lipid peroxidation was involved since these changes were blunted in IFN-gamma KO mice in response to the infection.

DISCUSSION

This study demonstrated that hypermetabolism following infection with *T. gondii* could not be explained by activation of sympathetic nervous system nor an increase in uncoupling protein 1 (UCP1) in the brown adipose tissue, a phenomenon that has previously been described following certain infections [7, 8].

Alternative mechanisms for hypermetabolism and lipid oxidation

In our model of toxoplasmosis, hypermetabolism was found to be associated with increased lipid oxidation, as assessed by a decrease in the respiratory quotient in the acute phase, as well as in the NG in the chronic phase. G showed a normalisation of RQ and a partial weight regain. Use of mercaptoacetate, which inhibits mitochondrial beta-oxidation did not increase and re-establish the RQ in the acute phase (day 4) and in the NG. This suggests the existence of extra-mitochondrial lipid oxidation. One alternative pathway could be an increased *in vivo* oxygen consumption *via* the activation of phagocytes including macrophages [21]. Indeed, the inhibition of oxidative burst by the NADPH oxidase (which produces ROS) by diphenyliodonium ablated the increase in VO2 following *in vivo* stimulation of phagocytes, without modifying mitochondrial activity significantly [21]. Macrophage oxidative burst may therefore account for a substantial component of the increase in oxygen consumption. Increases in ROS production by macrophages and enhanced lipid peroxidation have been shown to occur in various animal models of infection [22-24]. In our model there appears to be a shift in the location of ROS production and lipid peroxidation from the acute to the chronic phase of the infection. However in both phases, tissues with important macrophage or macrophage-like cells show the most significant increase in lipid peroxidation. It is important to note that NG produced more peroxidized lipids than G, suggesting enhanced oxidative stress in the NG.

It is well established that IFN-gamma is a major regulator of ROS in macrophages [25]. Infected IFN-gamma KO mice showed a marked reduction in their

hypermetabolic response and there was a decrease in their ROS production by peritoneal macrophages and attenuated lipid peroxidation (in sera, lungs, liver and spleen). High IFN-gamma levels are associated with hyperlipid peroxidation and cachexia in the chronic phase of the infection (*i.e.* in NG), the possibility arises that the mechanism maintaining cachexia resides in macrophage ROS production. Whether this increase in lipid peroxidation is beneficial [26] or not [27] remains to be substantiated.

Recently it has been shown that enhanced lipid entry into macrophage-type cells requires IFN-gamma [28] and that IFN-gamma increases LPL expression [29]. The blunted hypermetabolic response in the IFN-gamma KO mice may not only be due to decreased ROS production but also to reduce lipid uptake by phagocytic cells. Thus, IFN-gamma may not only increase the production of ROS but may also increase macrophage cellular uptake of lipids for oxidation, which would be consistent with a role of this cytokine in the lipid hypermetabolism seen in our model.

Infection or trauma can result in hypermetabolism, and in many of these cases there is also an increase in lipid peroxidation. The mechanisms described in our model may also be applicable to other injuries. Cerebral ischemia is accompanied by a strong inflammatory response, which is associated with a hypermetabolic state [30, 31] and enhanced lipid peroxidation component [32]. We have also been unable to attribute these effects to an elevation in BAT UCP1 expression in a murine model of cerebral ischemia [33], in fact in this model we also observed a decrease in UCP1 mRNA expression (data not shown). Increased lipid peroxidation by phagocytes may therefore be a major contributing factor to hypermetabolism in diseases. Whether IFN-gamma is the major regulator of this process in different infections and injuries remains to be determined, as does the role of the reactive oxygen species in body weight regulation.

CONCLUSION

Acknowledgements. The excellent assistance in preparation of article by Dr Adul Dulloo, Pierre Giguere, Julie Plamondon, Pierre Sampson, Raynald Schumacher, Prof. Josiane Seydoux and Philippe Vallet are gratefully acknowledged.

References

1. Rothwell N J. 1990. Mechanisms of pyrogenic actions of cytokines. (Review) *Eur. Cyt. Net.* 1: 211.

2. Rothwell N J. 1994. CNS regulation of thermogenesis. (Review) *Crit. Rev. Neurobiol.* 8: 1.

3. Rothwell N J. 1990. Neuroendocrine mechanisms in the thermogenic response to diet, infection and trauma. (Review) *Adv. Exp. Med.* Biol. 274: 371.

4. Luheshi G, Hopkins S J, Lefeuvre R A, Dascombe M J, Ghiara P, Rothwell N J. 1993. Importance of brain IL-1 type II receptors in fever and thermogenesis in the rat. *Am. J. Physiol.* 265: E585.

5. Cooper A L, Rothwell N J. 1991. Mechanisms of early and late hypermetabolism and fever after localized tissue injury in rats. *Am. J. Physiol.* 261: E698.

6. Arnold J, Little R A, Rothwell N J. 1989. Energy balance and brown adipose tissue thermogenesis during chronic endotoxemia in rats. *J. Appl. Physiol.* 66: 1970.

7. Cooper A L, Fitzgeorge R B, Baskerville A, Little R A, Rothwell N J. 1989. Bacterial infection *(Legionella pneumophilla)* stimulates fever, metabolic rate and brown adipose tissue activity in the guinea pig. *Life Sci.* 45: 843.

8. Cooper A L, Dascombe M J, Rothwell N J, Vale M J. 1989. Effects of malaria on O_2 consumption and brown adipose tissue activity in mice. *J. Appl. Physiol.* 67: 1020.

9. Arsenijevic D, Girardier L, Seydoux J, Chang H R, Dulloo A G. 1997. Altered energy balance and cytokine gene expression in a murine model of chronic infection with *Toxoplasma gondii. Am. J. Physiol.* 272: E908.

10. Arsenijevic D, Girardier L, Seydoux J, Pechere J C, Garcia I, Lucas R, Chang H R, Dulloo A G. 1998. Metabolic cytokine responses to a second immunological challenge with LPS in mice with *T. gondii* infection. *Am. J. Physiol.* 274: E439.

11. Nakane A, Numata A, Minagawa T. 1992. Endogenous tumor necrosis factor, interleukin-6 and gamma interferon levels during *Listeria monocytogenes* infection in mice. *Infect. Immun.* 60: 523.

12. Dalton D K, Pitts-Meek S, Keshav S, Figari I S, Bradley A, Stewart T A. 1993. Multiple defects of immune cell function in mice disrupted interferon-gamma genes. *Science* 259: 1739.

13. Pasparakis M, Alexopoulou L, Episkopou V, Kollias G. 1996. Immune and inflammatory responses in TNF-alpha-deficient mice : a critical requirement for TNF-alpha in the formation of primary B cell follicules, follicular dendritic cell networks and germinal centers and in the maturation of the humoral immune response. *J. Exp. Med.* 184: 1397.

14. Lowell B B, S-Susulic V, Hamann A, Lawitts J A, Himms-Hagen J, Boyer B B, Kozak L P, Flier J S. 1993. Development of obesity in transgenic mice after ablation of brown adipose tissue. *Nature* 366: 740.

15. Richard D, Chapdelaine S, Deshaies Y, Pepin MC, Barden N. 1993. Energy balance and lipid metabolism in transgenic mice bearing an antisense GCR gene construct. *Am. J. Physiol.* 265: R146.

16. Langhans W, Scharrer E. 1987. Evidence for a vagally mediated satiety signal derived from hepatic fatty acid oxidation. *J. Auton. Nerv. Syst.* 18: 13.

17. Arvaniti K, Ricquier D, Champigny O, Richard D. 1998. Leptin and corticosterone have opposite effects on food intake and expression of UCP1 mRNA in brown adipose tissue of lep (ob)/lep(ob) mice. *Endocrinolgy* 139: 4000.

18. Richard D, Rivest R, Huang Q, Bouillaud F, Sanchis D, Champigny O, Ricquier D. 1998. Distribution of the uncoupling protein 2 mRNA in the mouse brain *J. Comp. Neurol.* 397: 549.

19. Boss O, Samec S, Desplanches D, Mayet M H, Seydoux J, Muzzin P, Giacobino J P. 1998. Effect of endurance training on mRNA expression of uncoupling proteins 1, 2, and 3 in the rat. *FASEB J.* 12: 335.

20. Rook G A, Steele J, Umar S, Dockrell H M. 1985. A simple method for the solubilisation of reduced NBT, and its use as a colorimetric assay for activation of human macrophages by gamma-interferon. *J. Immunol. Methods* 82: 161.

21. Vlessis A A, Bartos D, Muller P, Trunkey D D. 1995. Role of reactive O_2 in phagocyte - induced hypermetabolism and pulmonary injury. *J. Appl. Physiol.* 78: 112.

22. Nishina M, Matsushita K, Furuhata T, Hori E, Takahashi M, Kato K, Matsuda H. 1994. Nuclear magnetic resonanace (NMR) analysis on the serum lipids of rabbits infected with *Schistoma japonicum*: oxidative modifications of the diene systems in fatty chains. *Int. J. Parasitol.* 24: 417.

23. Bergeron Y, Ouellete N, Deslauriers A M, Simard M, Olivier M, Bergeron M G. 1998. Cytokine kinetics and other host factors in response to pneumococcal pulmonary infection in mice. *Infect. Immun.* 66: 912.

24. Maffei Facino R, Carini M, Aldini G, Ceserani R, Casciarri I, Cavalletti E, Verderio L. 1993. Efficacy of glutathione for treatment of fascioliasis. An investigation in the experimentally infested rat. *Arzneimittelforschung.* 43: 455.

25. Nathan C F, Murray H W, Wiebe M E, Rubin B Y. 1983. Identification of interferon-gamma as the lymphokine that activates human macrophage oxidative metabolism and antimicrobial activity. *J. Exp. Med.* 158: 670.

26. Martynenko L D, Shepelev A P, Aleshukina A V. 1990. The effect of modulators of free radical oxidation on the functional activity of phagocytes Zh. *Mikrobiol. Epidemiol. Immunobiol.* 10: 113.

27. Tisdale M J. 1999. Wasting in cancer. (Review) *J. Nutr.* 129 (Suppl 1): 243S.

28. Whitman S C, Argmann C A, Sawyez C G, Miller D B, Hegele R A, Huff M W. 1999. Uptake of type IV hypertriglyceridemic VLDL by cultured macrophages is enhanced by interferon-gamma. *J. Lipid Res.* 40: 1017.

29. Garner B, Baoutina A, Dean R T, Jessup W. 1997. Regulation of serum induced lipid accumulation in human monocyte derived macrophages by interferon

gamma. Correlations with apolipoprotein E production, lipoprotein lipase activity and LDL receptor related protein expression. *Atherosclerosis* 128: 47.

30. Astrup J, Rehncrona S, Siesio B K. 1980. The increase in extracellular potassium concentration in the ischemic brain in relation to preischemic functional activity and cerebral metabolic rate. *Brain Research* 199: 161.

31. McCarthy H D, O'Saughnessy C T, Rothwell N J. 1989. Endogenous mediators of cerebral ischemia induced hypermetabolism in the rat. *Br. J. Pharmacol.* 98 (Suppl. I): 838P.

32. Coppi G. 1995. Neuroprotective activity of alpha - dihydroergcryptine in animal models. *J. Neural Transm. (Suppl.)* 45: 307.

33. de Bilbao F, Guarin E, Nef P, Vallet P, Giannakopoulos P, Dubois-Dauphin M. 2000. Cell death is prevented in thalamic fields but not in injured neocortical areas after permanent focal ischaemia in mice overexpressing the anti-apoptotic protein Bcl-2. *Eur. J. Neurosci.* 12: 921.

Figures

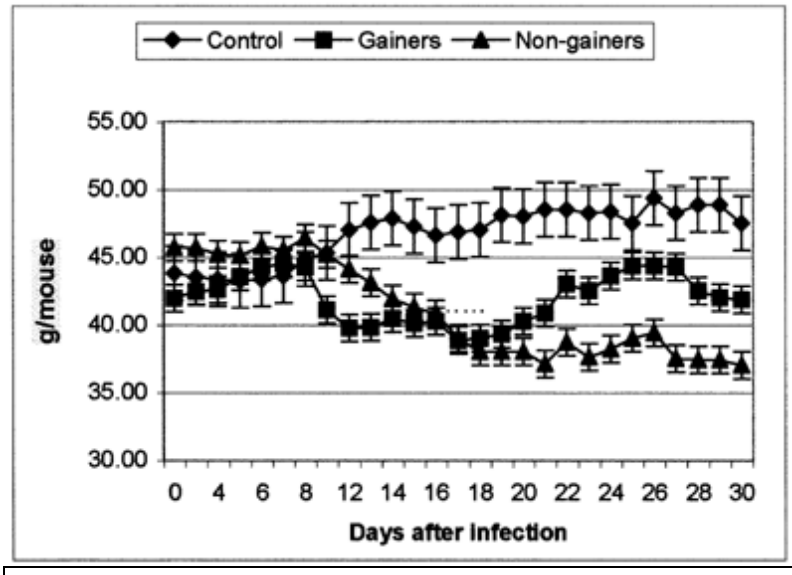


Figure 1
Profile of weight changes in Swiss Webster mice infected (i.p.) with 10 cysts of Toxoplasma gondii (Me49 strain).

Values are presented as mean ± SD for the various groups. After the weight loss phase, infected mice could be differentiated into those that showed persistant, although stable cachexia (Non Gainers) and those that showed a partial weight regain (Gainers). In this particular experiment 10 mice were infected, 4 become Gainers and 6 became Non Gainers.

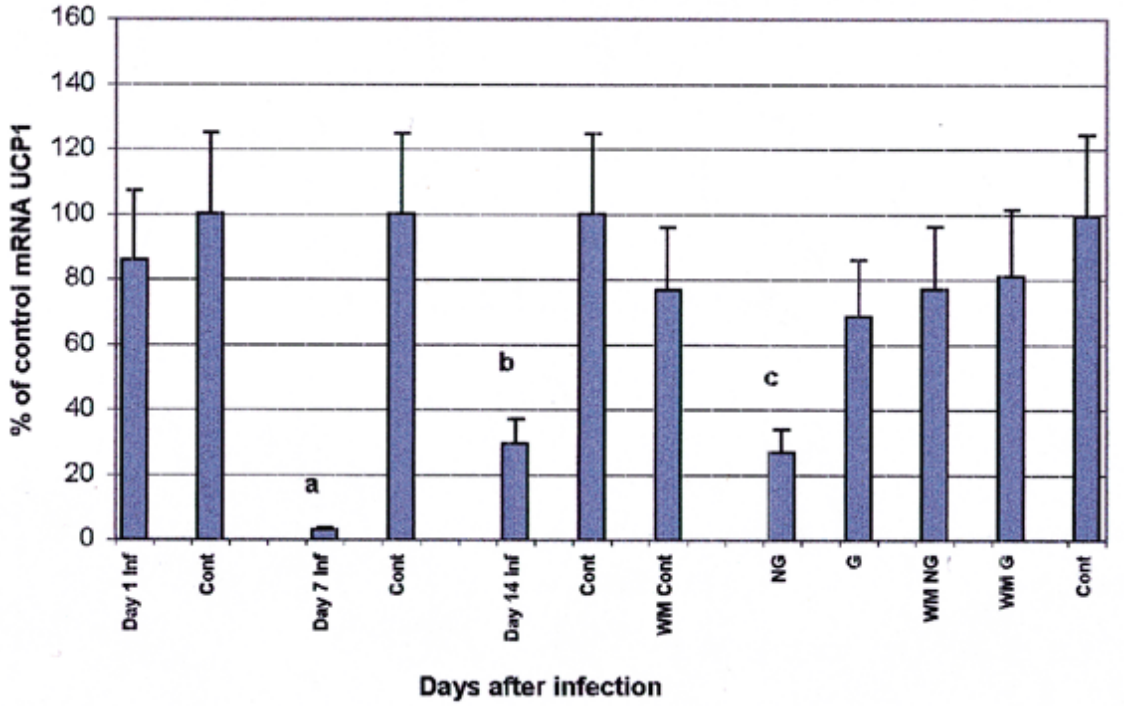


Figure 2

UCP1 mRNA levels in brown adipose tissue on various days after infection, UCP1 is given as a percentage of the control non-infected BAT in Swiss Webster.

On days 7, 14 and in NG the UCP1 levels in infected mice is significantly reduced ($p < 0.01$ (a), 0.01 (b) and 0.01 ©) respectively to controls. It is important to note that reduction in body weight as seen in the weight matched (WM) controls can result in a reduction in UCP1, which is independent of infection. Each value represents the mean of 5 mice.

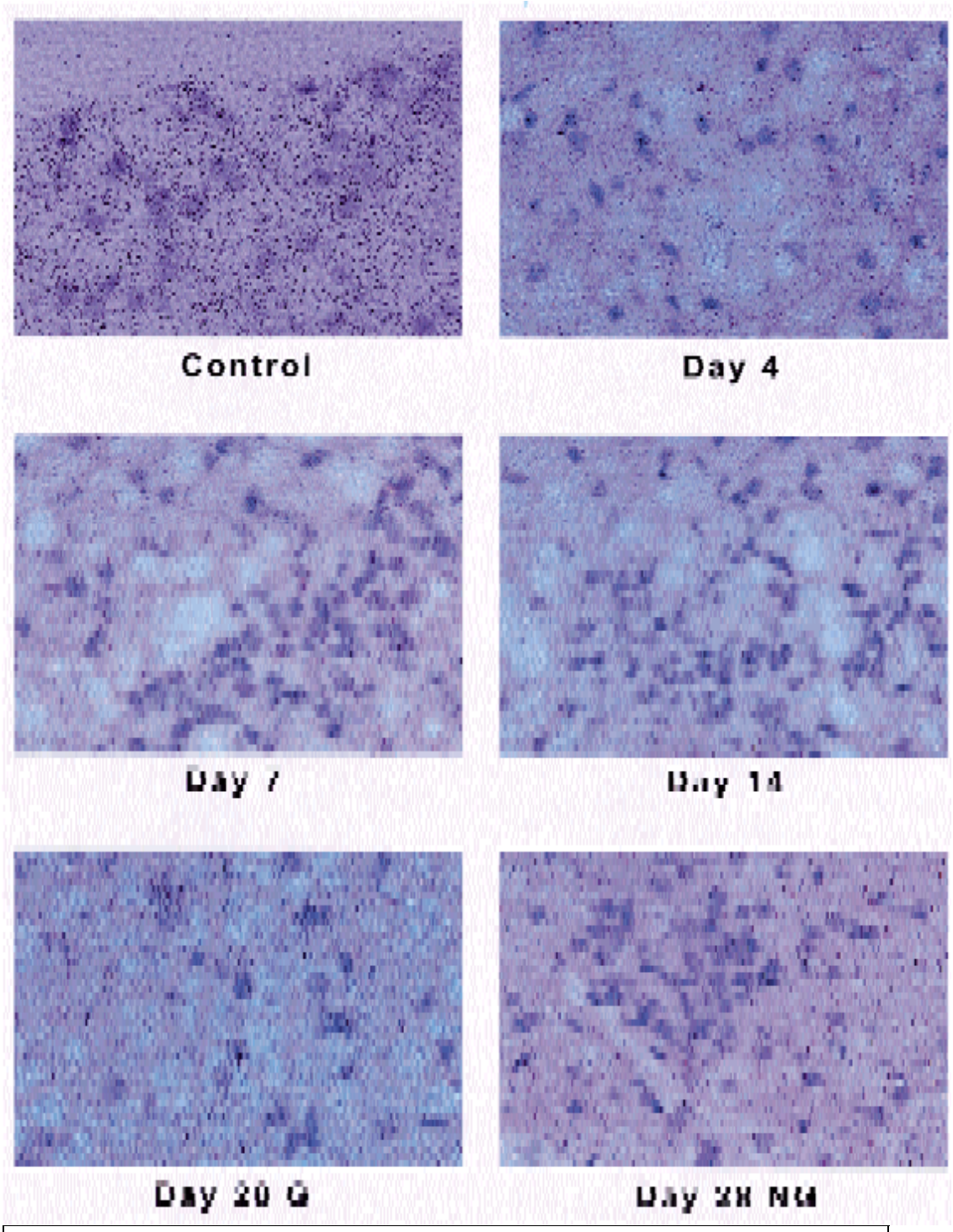
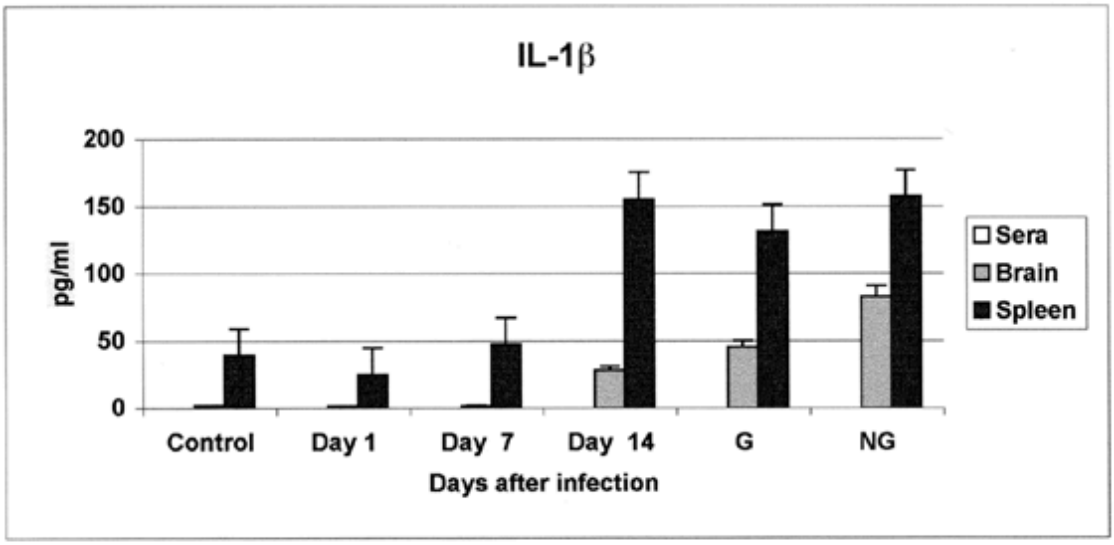
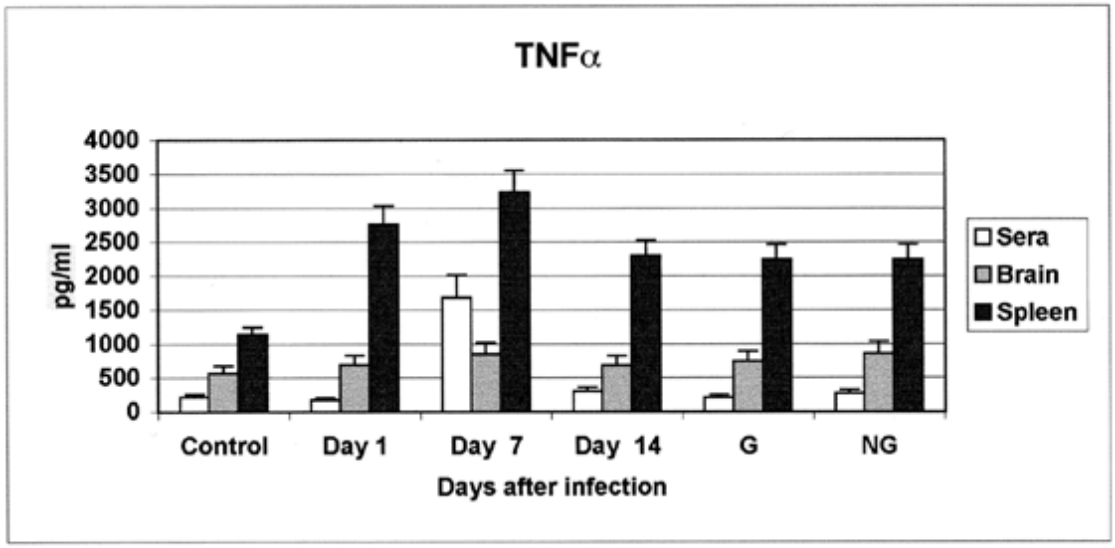


Figure 3
In situ **hybridization for UCP1 mRNA in brown adipose tissue in control mice (Control) and in infected mice on day 4, 7, 14 and 28 (in Gainers (G) and Non Gainers(NG)) with** ***Toxoplasma gondii.***

The control mice show more UCP1 labelling in the tissue than the infected group of mice. Note that UCP1 mRNA decreases following infection, this confirms our northern

blots for UCP1. These results are representative of observations made on brown adipose tissue in 4 mice in each group.





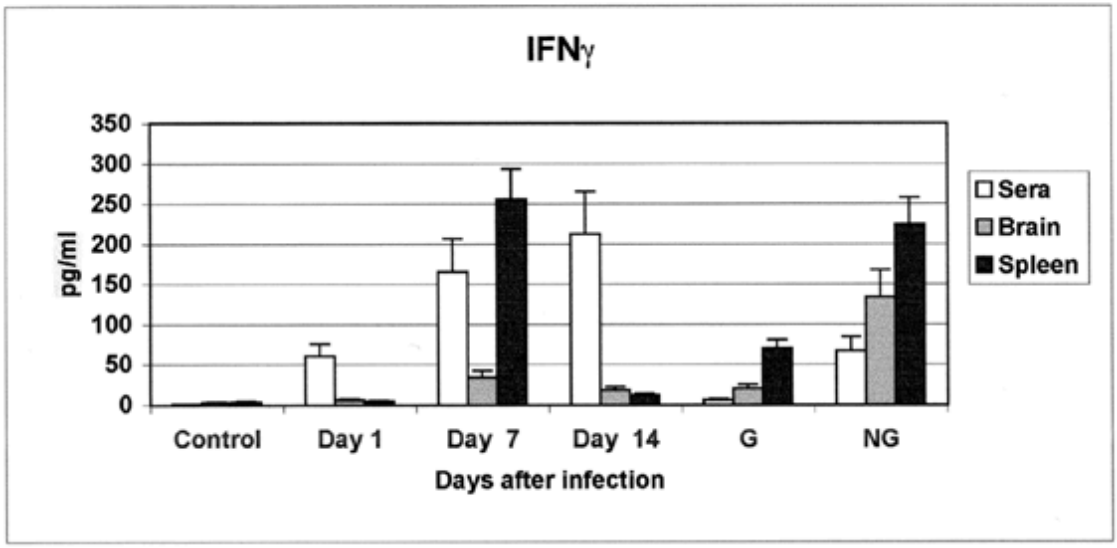
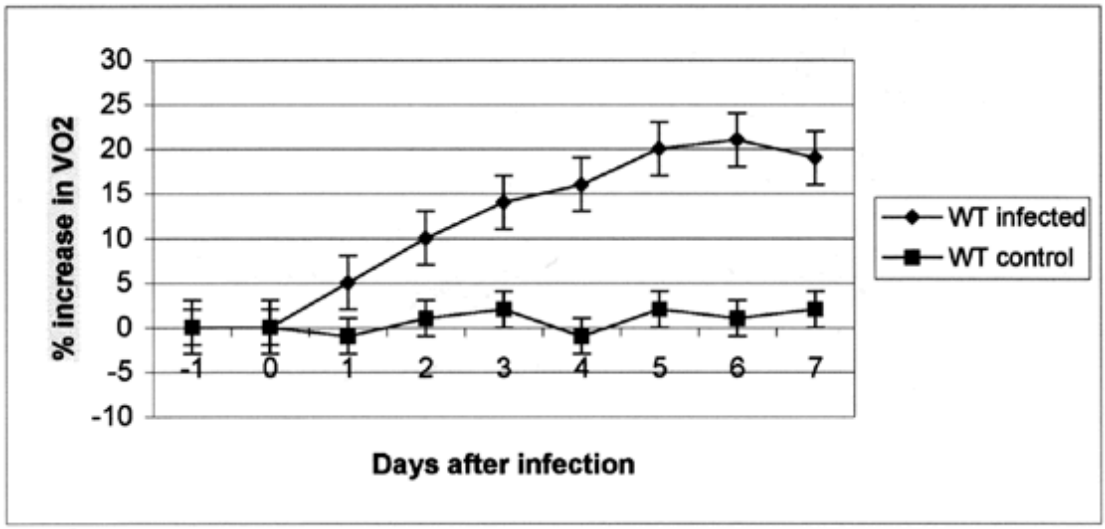
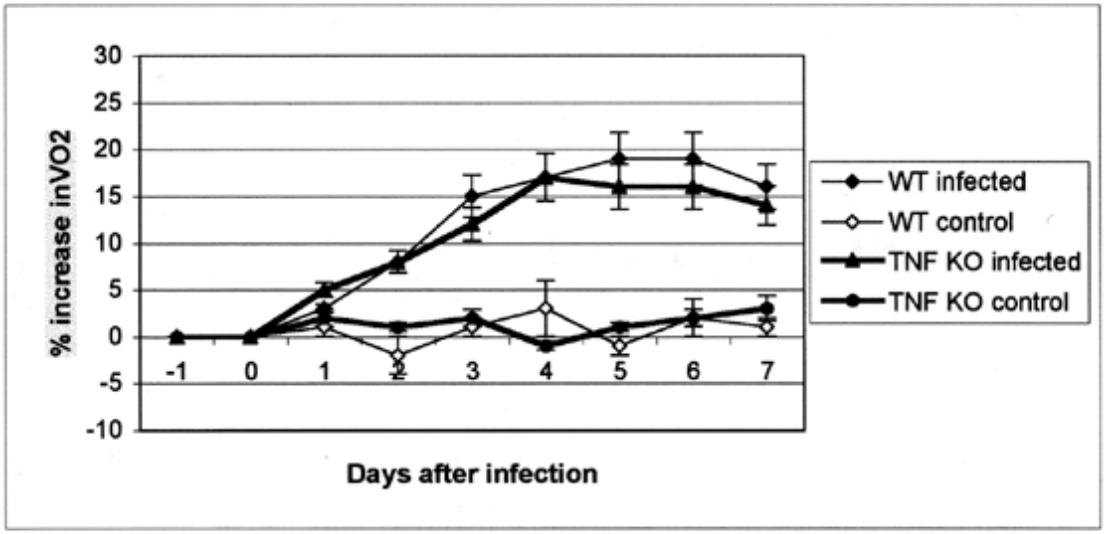


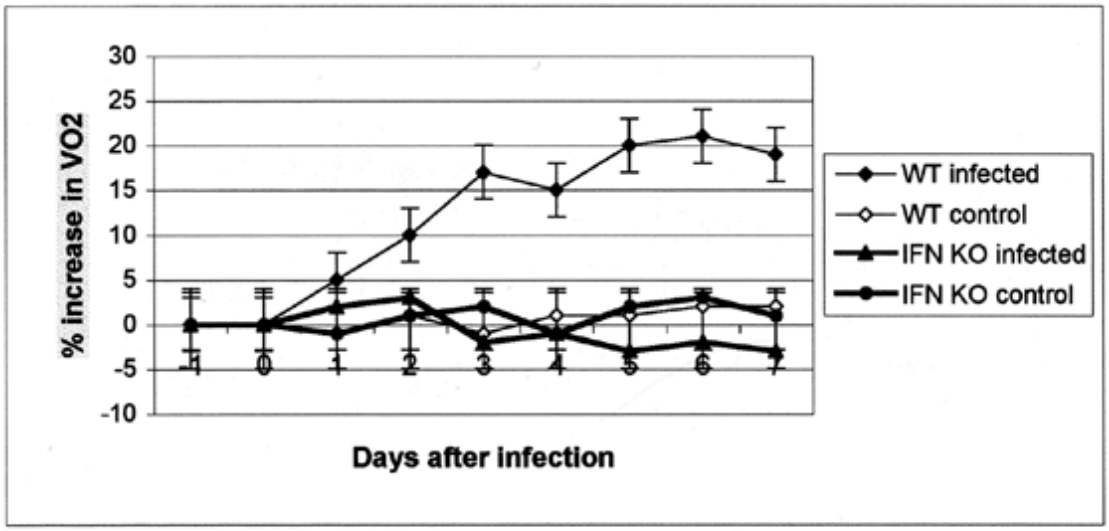
Figure 4

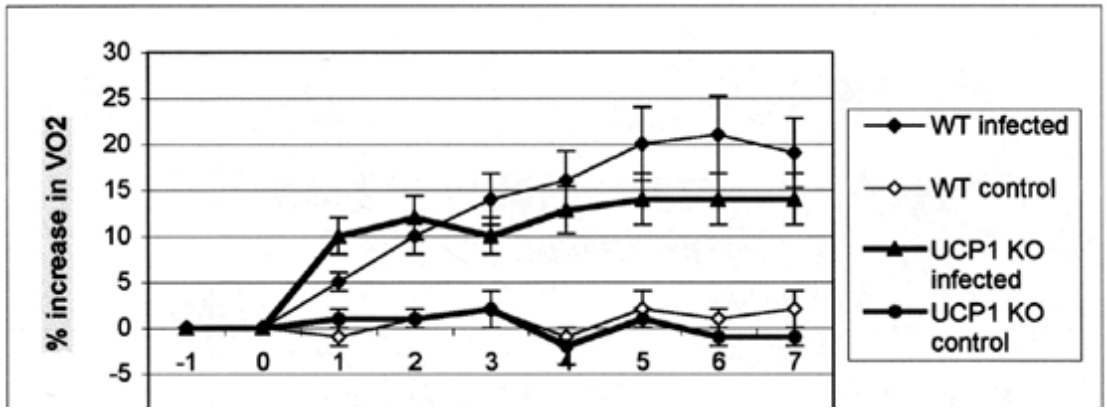
Serum, spleen and brain cytokine concentrations at various days following ip infection with 10 cysts of *Toxoplasma gondii.*

The values are the mean ± SD (n = 3). IL-1beta, TNF-alpha and IFN-gamma were measured by immunoassays as described in the methods and material section. Note that IFN-gamma shows a better association with the hypermetabolic response than the other two cytokines following infection.


% increase in VO2
30
25
20
15
10
5
0
-5
-10
-1
0
1
2
3
4
5
6
7
Days after infection
WT infected
WT control


% increase inVO2
30
25
20
15
10
5
0
-5
-10
-1
0
1
2
3
4
5
6
7
Days after infection
WT infected
WT control
TNF KO infected
TNF KO control


% increase in VO2
30
25
20
15
10
5
0
-5
-10
Days after infection
WT infected
WT control
IFN KO infected
IFN KO control


% increase in VO2
30
25
20
15
10
5
0
-5
-1
0
1
2
3
5
6
7
WT infected
WT control
UCP1 KO infected
UCP1 KO control

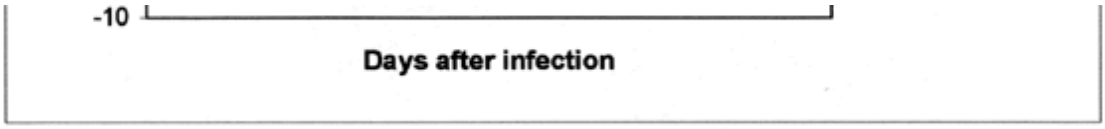


Figure 5

Hypermetabolic response (VO2 increase) in different mouse strain following ip infection with 10 cysts of *Toxoplasma gondii* during the first week of infection.

VO2 increase in Swiss Webster mice (Top panel), TNFalpha KO and their WT counterparts of C57BL/6 background (2nd panel), IFN-gamma KO and their WT counterparts Balb/c background (3rd panel) and UCP1 KO and their FVB NJ WT counter parts (4th panel). All mice show a maintained increase in VO2 after infection with the exception of IFN-gamma KO mice. For each group (n = 4 mice) VO2 was determined as described in the methods and material section.

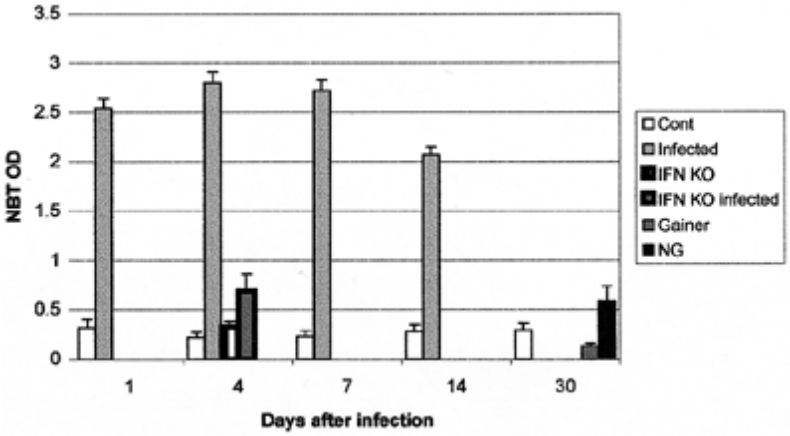


Figure 6

NBT reduction by peritoneal macrophage on days 1, 4, 7, 14 and day 30 after ip infection with 10 cysts of *Toxoplasma gondii.*

WT mice show an increase in NBT reduction by peritoneal macrophages while IFN-gamma KO mice have a markedly attenuated response on day 4 post infection. Number of animals per group: n = 3.

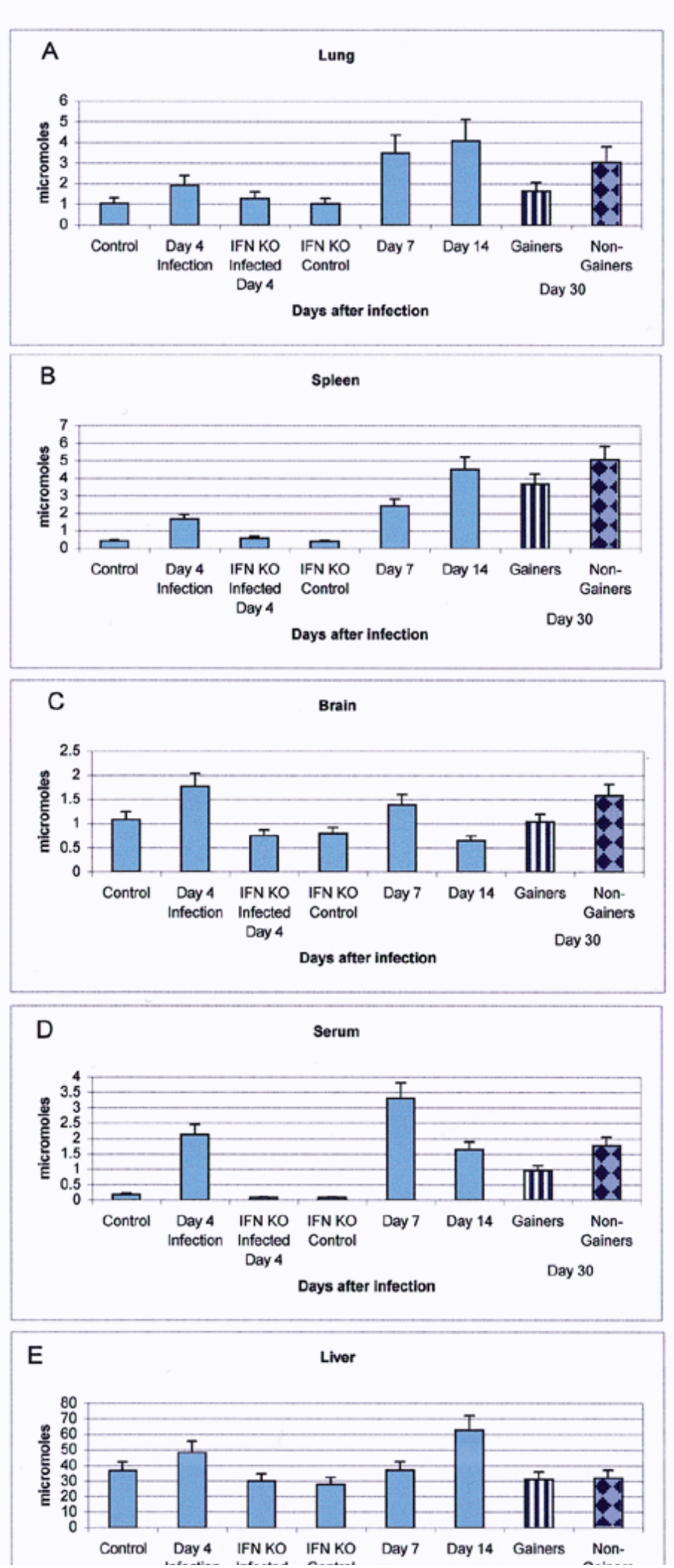

A
Lung
micromoles
0
1
2
3
4
5
6
Control
Day 4 Infection
IFN KO Infected Day 4
IFN KO Control
Day 7
Day 14
Gainers
Non-Gainers
Day 30
Days after infection
B
Spleen
micromoles
0
1
2
3
4
5
6
7
Control
Day 4 Infection
IFN KO Infected Day 4
IFN KO Control
Day 7
Day 14
Gainers
Non-Gainers
Day 30
Days after infection
C
Brain
micromoles
0
0.5
1
1.5
2
2.5
Control
Day 4 Infection
IFN KO Infected Day 4
IFN KO Control
Day 7
Day 14
Gainers
Non-Gainers
Day 30
Days after infection
D
Serum
micromoles
0
0.5
1
1.5
2
2.5
3
3.5
4
Control
Day 4 Infection
IFN KO Infected Day 4
IFN KO Control
Day 7
Day 14
Gainers
Non-Gainers
Day 30
Days after infection
E
Liver
micromoles
0
10
20
30
40
50
60
70
80
Control
Day 4
IFN KO
IFN KO
Day 7
Day 14
Gainers
Non-



Figure 7

Amount of lipid peroxidation as determined by colorimetric assay as described in the methods and material section, in the lung, spleen, liver, brain and serum after ip infection with 10 cysts of *Toxoplasma gondii.*

Figures show the amount of lipid peroxidation in various tissues in the chronic phase of the infection, note that in all tissues examined lipid peroxidation is always greater in NG than G and controls. Figures show the importance of IFN-gamma in the process of lipid peroxidation following infection, since on day 4, infected mice have increase a lipid peroxidation in all tissues, while at this same time point IFN-gamma KO mice show no significant increase in all tissues assisted ($p < 0.01$) and the latter were similar to non infected controls $p < 0.01$. Number of animals per group $n = 3$.

Table 1
Respiratory Quotient (RQ) and the dependence on cytokines using TNF and IFN-gamma knockout mice following infection

Mouse (n = 4)	RQ	Kruskal-Wallis non parametrical one way AOV
Cytokine knockouts		
WT	0.93 ± 0.02	0.02
WT infected day 4	0.85 ± 0.02	
IFN KO	0.91 ± 0.01	NS
IFN KO infected day 4	0.92 ± 0.02	
TNF KO	0.92 ± 0.02	0.02
TNF KO infected day 4	0.86 ± 0.02	
UCP1 KO	0.88 ± 0.01	0.02
UCP1 KO infected Day 4	0.84 ± 0.01	
WT	0.94 ± 0.01	0.01
WT infected day 7	0.78 ± 0.02	
WT	0.93 ± 0.02	0.01
WT infected day 14	0.79 ± 0.06	
WT	0.91 ± 0.02	NS
Day 28 G	0.94 ± 0.02	
WT	0.89 ± 0.02	0.01
Day 28 NG	0.77 ± 0.02	

Authors

D. Arsenijevic, F. de Bilbao, P. Giannakopoulos, L. Girardier, S. Samec, D. Richard

Physiology and Animal Husbandary, Institute of Physiology and Animal Science, Swiss Federal Institute of Technology Zurich, Schorenstrasse 16, Schwerzenbach 8603, Switzerland

In this issue

Virus-cell interactions: impact on cytokine production, immune evasion and tumor growth

T. H. Mogensen, S. R. Paludan
virus, cytokines, signal transduction, immune evasion, tumor growth.

Safety, pharmacokinetics and pharmacodynamics of recombinant human tumour necrosis factor-binding protein-1 (Onercept) injected by intravenous, intramuscular and subcutaneous routes into healthy volunteers

I. Trinchard-Lugan, Q. Ho-Nguyen, W.M. Bilham, M. Buraglio, A. Ythier, A. Munafo
recombinant human tumour necrosis factor-binding protein-1 (r-hTBP-1), safety, pharmacokinetics, pharmacodynamics.

Direct effects of tumor necrosis factor alpha (TNF-alpha) on murine skeletal muscle cell lines. Bimodal effects on protein metabolism

B. Alvarez, L. S. Quinn, S. Busquets, F. J. López-Soriano, J. M. Argilés
cytokines, myotubes, cachexia, protein turnover.

Receptor-like properties of the 26 kDa transmembrane form of TNF

A. Domonkos, A. Udvardy, L. László, T. Nagy, E. Duda
cytokine, TNF family, receptor, signaling, reverse-signaling.

Local administration of interleukin-1beta for the treatment of lung abscesses induces neutrophil activation and changes in proinflammation cytokine production

A. Simbirtsev, E. Variouchina, V. Konusova, A. Kotov, S. Ketlinsky, A. Salamatov, L. Bisenkov
recombinant human interleukin-1beta, lung inflammation, abscess, neutrophils, cytokines.

Effects of interleukin-2 therapy on the proliferation and differentiation of CD4/CD25 positive and CD4/CD25 negative cells in HIV+ patients

L. Caggiari, S. Zanussi, M. D'Andrea, M. T. Bortolin, C. Crepaldi, C. Caffau, P. de Paoli
cytokines, Ki67, intracellular IFN-gamma.

Tumor necrosis factor-alpha and nitric oxide in vertically HIV-1-infected children: implications for pathogenesis

J. González-Nicolás, S. Resino, J. L. Jiménez, S. Alvarez, M. Fresno, M. A. Muñoz-Fernández
tumor necrosis factor, nitric oxide, HIV-infection, immunological and virological markers.

Serum levels of angiogenic cytokines in systemic lupus erythematosus and their correlation with disease activity

E. Robak, A. Wozniacka, A. Sysa-Jedrzejowska, H. Stepien, T. Robak
systemic lupus erythematosus, disease activity, angiogenesis, platelets, hepatocyte growth factor, vascular endothelial growth factor, basic fibroblast growth factor, transforming growth factor beta.

Modulation of the allergen-induced human IgE response in Hu-SCID mice: inhibitory effect of human recombinant IFN-gamma and allergen-derived lipopeptide

C. Duez, H. Gras-Masse, H. Hammad, H. Akoum, A. Didierlaurent, C. André, A.-B. Tonnel, J. Pestel
SCID mouse, IgE, IFN-gamma, lipopeptide, house dust mite.

Cytokine-inducing activity of a proline-rich polypeptide complex (PRP) from ovine colostrum and its active nonapeptide fragment analogs

A. Zablocka, M. Janusz, K. Rybka, I. Wirkus-Romanowska, G. Kupryszewski, J. Lisowski
ovine colostrum, proline-rich polypeptide complex (PRP), nonapeptide (NP) and hexapeptide (HP) from PRP, oligomers of NP and HP, cytokines.

Quantitation of chemokines (MDC, TARC) expression in mucosa from Crohn's disease and ulcerative colitis

F. Jugde, M. Alizadeh, C. Boissier, D. Chantry, L. Siproudhis, S. Corbinais, E. Quelvennec, F. Dyard, J.-P. Campion, M. Gosselin, J.-F. Bretagne, G. Sémana, D. Heresbach
real-time TR-PCR, chemokines, Crohn’s disease, ulcerative colitis.

Activation of caspase-3 by interferon alpha causes interleukin-16 secretion but fails to modulate activation induced cell death

O. Ludwiczek, A. Kaser, R. O. Koch, W. Vogel, W. W. Cruikshank, H. Tilg

interleukin-16, interferon-alpha, caspase-3.

Cytokine deviation induced by intrathymic injection of staphylococcal enterotoxin B (SEB)

P. Goettelfinger, F. Lecerf, S. Berrih-Aknin, M. German-Fattal
SEB, intrathymic injection, anergy, cytokine deviation, quantitative RT-PCR.

Strain-dependent difference in inducible nitric oxide synthesis (iNOS) expression in rat pancreatic islets correlates with interferon regulating factor 1 (IRF-1) and heat shock protein 70 (HSP70) expression

J. Johannesen, F. Pociot, A. E. Karlsen, T. Mandrup-Poulsen, J. Nerup
type 1 diabetes, islets of Langerhans, beta-cells, cytokines, interleukin-1beta, interleukin-1beta receptor type I, nitric oxide, inducible nitric oxide synthase, heat shock protein 70, interferon regulating factor 1.

Neutrophil apoptosis in autoimmune Fas-defective MRL lpr/lpr mice

E. Del Giudice, A. Ciaramella, N. Balestro, D. Neumann, P. G. Romano, M. P. Cesaroni, G. Maurizi, P. Ruggiero, D. Boraschi, P. Bossù
neutrophils, apoptosis, autoimmunity.

A role for interferon-gamma in the hypermetabolic response to murine toxoplasmosis

D. Arsenijevic, F. de Bilbao, P. Giannakopoulos, L. Girardier, S. Samec, D. Richard
toxoplasma, hypermetabolism, reactive oxygen species, lipid peroxidation, UCP1, interferon-gamma.

Protection of mice from malaria after co-administration of recombinant mouse granulocyte-macrophage colony-stimulating factor and methionine-enkephalin

P. Pal Singh, S. Singh
Plasmodium berghei, protection, rmGM-CSF, met-enkephalin.

Semiautomated and simultaneous analysis of the interleukin-10 gene microsatellites IL-10G and IL-10R by fluorescence-based polymerase chain reaction reveals significant differences in allele distributions between Caucasians (Germany) and Africans (Gabon)

D. Kube, D. Schmidt, M. Mörmann, A.C. Uhlemann, J. Tomiuk, H. Tesch, P.G. Kremsner

microsatellites, interleukin-10 promoter, multiplex-PCR, Caucasian, African.

Les éditions JLE

30 rue Berthollet, Bât. A,
94110 Arcueil, France

+ 33 (0)1 46 73 06 60

contact@jle.com

Publishing Policy

Books and e-books

Want to publish ?

Become a partner







